Frequency Analysis of Amide-Linked Rotaxane Mimetics

Werner Reckien, Barbara Kirchner, and Sigrid D. Peyerimhoff*

Theoretische Chemie, Institut für Physikalische und Theoretische Chemie, Universität Bonn, Wegelerstr. 12, D-53115 Bonn, Germany

Received: August 17, 2006; In Final Form: September 28, 2006

A vibrational analysis of 2-fold hydrogen bonds between an isophthalic amide donor and different acceptors is presented. These systems can be considered as mimetics for the hydrogen-binding situation of numerous supramolecular compounds such as rotaxanes, catenanes, knotanes, and anion receptors. We calculated pronounced red-shifts up to 65 cm^{-1} for the stretching modes of the acceptor carbonyl as well as for the donor NH_2 groups, whereas we observe a blue shift for the NH_2 bending modes and an additional weak hydrogen bond between the acceptor and the middle C−H group of the donor. The red and blue shifts observed for different modes in various complexes have been correlated with the binding energy of the complexes, independently. In comparison with comparable single hydrogen bonds, we find for the 2-fold hydrogen bonds smaller red shifts for the N−H stretch modes of the donor but larger red shifts for the C═O stretch mode of the acceptor. Furthermore, our results indicate that the pronounced blue shift of the C−H stretch mode is basically caused by the fact that the acceptor is fixed directly above this group due to the 2-fold hydrogen bond.

1. Introduction

Rotaxanes are supramolecular systems which consist of a macrocyclic compound (wheel or ring) threaded onto a linear molecule (axle). They are of special interest, because they have some freedom of motion; that is, the wheel can rotate or slide along the axle depending on the chemical environment, oxidation state, temperature, and so on. These kind of supramolecules are expected to be key compounds in the design of molecular machines. The two components of the rotaxane are not connected via covalent bonds, but bulky terminal stoppers at both ends of the axle prevent the ring from dethreading. A magic glue between the two units of a rotaxane that allows for the complicated dynamics is hydrogen bonds in several varieties. The possibilities are reflected in the strength with which hydrogen-bonded complexes are held together and in their geometries.[1−5] Indeed weak intermolecular interactions such as hydrogen bonds or $\pi-\pi$ stacking interactions play a pivotal role in rotaxane chemistry: The synthesis of rotaxanes and similar compounds such as catenanes and knots proceeds in many cases only by template effects based on these interactions.[6−13]

Hydrogen-bonded complexes X−H···Y can vary in donor X and acceptor Y atoms or groups.[1,14,15] The donor atom X is generally thought to be electronegative (for example O or N) as is the proton acceptor Y.[16,17] In a classical picture, the electron density of Y exerts an attractive force on the proton, and as a result, the X−H bond should lengthen which can be observed in a red shift of the X−H frequency. On the other hand very weak hydrogen bonds[5] can also be formed with a carbon atom being the donor atom instead of the more electronegative oxygen or nitrogen atom. For such hydrogen bonds, it is found that the X−H stretching vibration is shifted toward higher frequency (blue-shift) in an X−H···Y hydrogen-bonded system.[18−25] Theoretical discussions concerning this weak or blue-shifted hydrogen bond were carried out in extenso by the Hobza group.[23,26,27] The term "anti-hydrogen bond" or "improper hydrogen bond" was coined in order to discuss the different nature of this hydrogen bond.[23,26,27] As opposed to this, Scheiner and co-workers point out that this hydrogen bond is not so special and that only the weights for the different contributions adding up to the hydrogen bonding are differently distributed in the blue-shifted and in the red-shifted hydrogen bonds.[28−30] Li et al. analyze blue-shifted hydrogen bonds and come to the conclusions that the balance between attractive and repulsive interactions is present in both types (regular red-shifted and abnormal blue-shifted) of hydrogen bonds but to a different proportion and conclude that both the blue-shifted as well as the red-shifted hydrogen bonds are governed by the same interactions.[19] Furthermore Dannenberg and co-workers ascribe the shortening of the C−H bond to the electric field of the acceptor which effectuates that electron density moves from the hydrogen into the C−H bond.[31] In this context Hermansson has shown that the dipole moment derivative with respect to the C−H stretching coordinate can explain the observed blue shifts.[32] Alabugin et al. ascertain that blue shifted hydrogen bonds are a consequence of Bent's rule[33] which predicts an increase in the s character of the X-hybrid atomic orbital of the X−H donor group upon hydrogen bond formation.[34] Other investigations support this point of view based on the observation that a linear relationship exists between the properties derived from the electron densities or the density itself and the interaction energy of the hydrogen-bonded complex.[15,35−41] Ab initio calculations for hydrogen-bonded systems have been carried out first by Morokuma and Pedersen for the dimeric $H_2O\cdots H_2O$.[42] In the early nineties, the excited states spectrum and the IR-frequency spectrum were determined for a series of hydrogen-bonded complexes involving formaldehyde.[43,44]

Recently, we have analyzed the importance of the 2-fold hydrogen-bonded systems as model compounds of the hydrogen bond situation in amide-linked rotaxanes.[38] In the present work, we extend this study of the 2-fold hydrogen bond to the investigation of the IR-spectroscopic properties with a focus

10.1021/jp065327m CCC: $33.50
Published on Web 11/09/2006

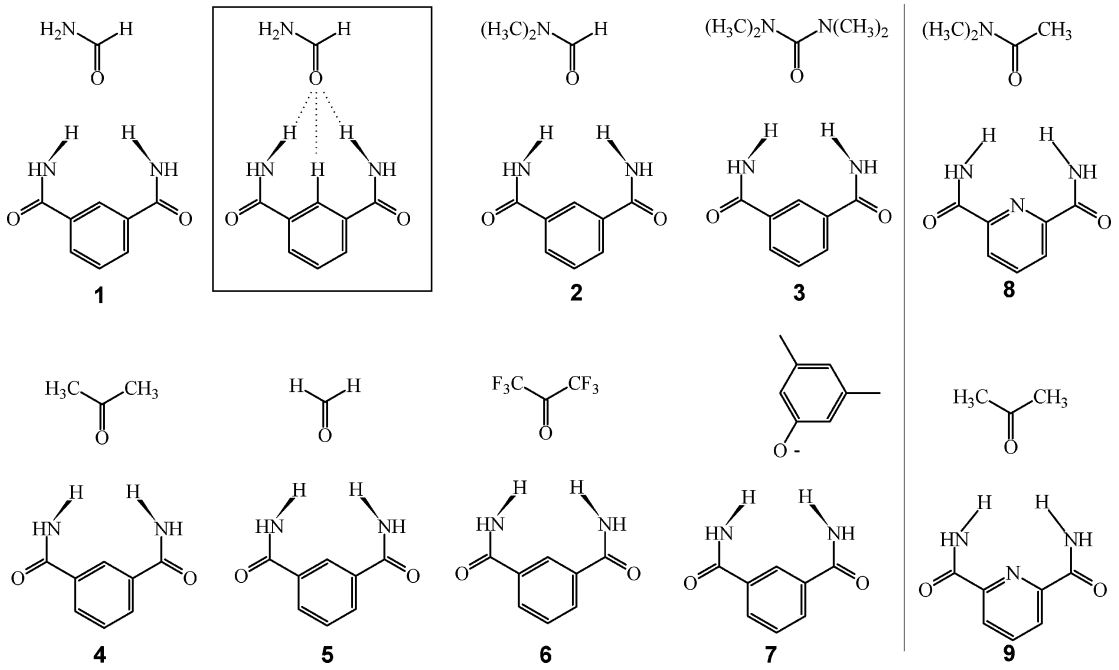

Figure 1. Two-fold hydrogen bond complexes with different donor and acceptor molecules. The scheme of complex **1** within the extra frame shows the possible N−H and C−H contacts between donor molecule and acceptor molecule.

on the carbonyl N−H···O hydrogen bond. This was done because vibrational spectroscopy enables an important microscopic access to the microscopic aspects of hydrogen bonds in complex systems.[45−52] In addition, we investigate possible weak C−H···O bridges and their IR-frequency dependence on substitutional effects. In particular, amide hydrogen bonds which do not only play a role in supramolecular template effect but also in peptide bonds were subject of detailed investigations.[53−61] However, the special spectroscopic properties of 2-fold hydrogen bridges, where one (amide) acceptor builds up two hydrogen bonds to an (isophthalic amide) donor are not well investigated yet. Our vibrational analysis will contribute to a better understanding of such hydrogen bonds and may be useful for detection and interpretation of hydrogen bonds in experiments especially in light of supramolecular chemistry[45,62−65] and as mimetic for the above-mentioned rotaxanes.

The article is organized as follows. First we describe the methodologies and programs used. Next we introduce the systems investigated with a subsequent discussion of geometrical parameters. After this we discuss the vibrational frequencies that are relevant for hydrogen bonding. We finish this article with a discussion and conclusions.

2. Methodology

We present an analysis of vibrational frequencies in model systems for the 2-fold hydrogen bridges in amide-templated rotaxanes and knots as synthesized by Vögtle, Schalley, Leigh, and others.[6,8,9,13,66] For this purpose, we perform density functional calculations of selected systems which were already examined in a previous study.[38]

All calculations are carried out employing the DFT method with the B3LYP[67,68] functional in a TZVP[69] basis as implemented in the TURBOMOLE 5.6 suite.[70] At first we reoptimize structural parameters of the systems compared to the treatment in our previous work with a threshold for the norm of the gradient of 10^{-4}. The SCF convergency criterion for these calculations is chosen as 10^{-8}. For the frequency analyses, the program package SNF[71] was employed. The second derivatives of the total electronic energy of the harmonic force field are calculated numerically with energy gradients of distorted structures, which were obtained from TURBOMOLE calculations. According to the $O(h^2)$ truncated error of the 3-point central-difference formula used for the first derivative (with a step size $h = 0.01$ bohr), we obtain a four-figure numerical accuracy. The numerical accuracy of the calculated wavenumbers is thus not below 1 cm^{-1}. We do not apply scaling factors for a readjustment of the calculated frequencies. Dipole moments were calculated according to the Davidson−Roby−Ahlrichs population analysis as implemented in the TURBOMOLE 5.6 suite.[70] For the one anionic system in this study, see section 3, we did not add diffuse functions as previously,[38] because the emphasize here is not on this system. The consideration of diffuse functions leads in this case only to a small lowering (about 1 kJ/mol) of the interaction energy. We added this one system only for the sake of comparison.

3. Systems Investigated

The systems investigated are the isophthalic amide (in the following abbreviated **IA**) hydrogen bond complexes **1** to **6** and **7**, see Figure 1. All have the same 2-fold hydrogen bond donors, while the acceptor molecules are varied. It has previously been found that electron donating substituents such as methyl groups instead of amide hydrogens as in **2** and **3** increase the interaction energy. Reduction of the interaction energies can be expected if the electron donating NH_2 group is replaced by hydrogen atoms or alkyl groups such as CH_3. These trends are closely related to the charges on the carbonyl oxygen atom that accepts the two hydrogen bonds.[38] System **7** is not directly comparable to the other complexes, because **7** does not involve a doubly bonded carbonyl oxygen but a single bonded phenolate group which is negatively charged. However, this acceptor is interesting, because many rotaxanes contain such a building block at the axle to bind to the wheel[9−12,72,73] and because comparable isophthalic amides are found to be excellent neutral anion receptors.[74−78] Furthermore, we investigated systems **8** and **9** because in some rotaxanes and knotanes 2-fold hydrogen bonds to a 2,6-pyridinedicarboxamide moiety (**PC**) are observed. To gain further insight into the nature of the 2-fold hydrogen-

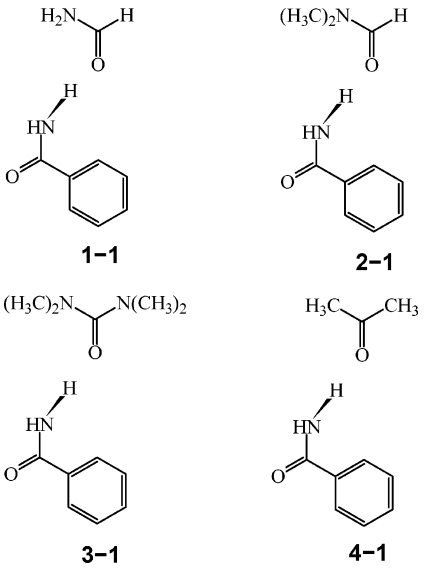

Figure 2. One-contact hydrogen bond complexes with different acceptor molecules and the benzamide (abbreviated **BA** in the following) as donor molecule.

bonded complexes, comparable systems with single hydrogen bridges are studied for comparison. These are shown in Figure 2.

4. Results

4.1. Geometries and Energies. In Table 1, we list the hydrogen bond parameters as obtained from optimization for the structures of the complexes shown in Figure 1 and discussed previously.[38] The isophthalic amide **IA** contains two amide groups, which are not distinguishable by the chemical environment. Therefore, we distinguish the first amide group as the one with the shorter hydrogen bond (in case they are different) from the second that is the one with the longer hydrogen bond. In Figure 1, the complexes appear very symmetrical; however, after optimization, not all complexes orient spatially in a symmetrical (planar) way in particular the large groups at the acceptor molecule show a tendency to arrange in such a way to minimize repulsion, which is reflected in the different lengths of the amide hydrogen bonds. We obtain hydrogen bond parameters with the acceptor−donor distance smaller than 350 pm and the acceptor−proton−donor angle mostly larger than 170°, only in complex **6** we find smaller angles of 159.3° and 159.1° respectively. These trends are in accordance with the previous study in which we also present results of MP2 calculations for these systems.[38] The donor−acceptor distances are systematically by 2 to 3 pm longer in the present study than previously which is due to the different functional and basis set (now B3LYP/TZVP, previously BHLYP/TZP).

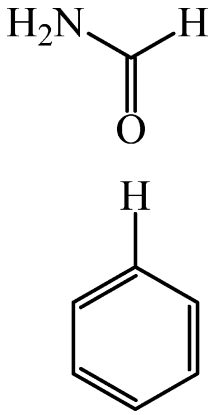

Figure 3. Weak hydrogen bond. This complex was obtained from **1** by replacing the amide groups of the aromatic ring of the donor by hydrogen atoms. It has a calculated interaction energy of 2 kJ/mol.

We also observe a third contact, namely a weak hydrogen bond to the C−H group as indicated in Figures 1 and 3. Surprisingly, these hydrogen-bond-like contacts exhibit also an ideal acceptor−donor distance of less than 350 pm (364 pm for **6**). In general the O···C distance is longer by roughly 10 pm than the O···N separation. The calculated hydrogen bond angles C−H···O are smaller than 148° and deviate much from the ideal linear arrangement. Such ranges of angles are well-known for the weak C−H···O hydrogen bonds.[5] The interaction energies are between −7 and −43 kJ/mol being therefore in the range of 1/2−2 hydrogen bonds in ordinary water (E_I(water

TABLE 1: Geometry Parameters (Distances *R* in pm and Angles *A* in Degrees) and Energies (in kJ/mol) for the 2-Fold and Single Bonded Complexes[a]

	1. amide group			2. amide group			C−H···O				
	R_{ON}	A_{OHN}	ΔR_{NH}	R_{ON}	A_{OHN}	ΔR_{NH}	R_{OC}	A_{OHC}	ΔR_{CH}	E_I	E_I^{ZPE}
					2-Fold Bonded						
3	316.3	175.0	0.6	318.5	177.4	0.6	328.3	147.5	−0.4	−43.2	−39.6
2	320.4	175.3	0.5	322.3	177.4	0.5	331.5	141.0	−0.4	−37.9	−33.7
1	323.5	177.5	0.4	320.7	175.7	0.4	333.1	141.0	−0.3	−35.8	−30.5
4	324.5	176.7	0.4	325.0	176.6	0.4	336.1	139.0	−0.3	−31.6	−28.0
5	331.4	173.9	0.3	331.4	173.9	0.3	345.5	140.7	−0.3	−24.0	−18.2
6	344.7	159.3	0.1	344.8	159.1	0.1	364.4	142.8	−0.1	−6.6	−4.9
7	292.0	174.9	2.6	292.1	177.5	2.6	298.8	152.7	−0.4	−155.9	
8	308.2	156.5	0.7	309.7	156.3	0.6				−31.2	−25.4
9	315.1	156.5	0.5	315.7	155.2	0.5				−23.6	−21.5
					Single Bonded						
3-1	299.1	169.8	0.7				344.4	159.0	−0.1	−26.7	−23.2
2-1	302.7	170.4	0.6				347.3	148.5	−0.1	−24.6	−21.1
1-1	306.0	169.4	0.5				348.2	161.4	−0.1	−22.5	−17.8
4-1	310.0	169.5	0.4				353.5	152.5	−0.1	−19.6	−16.9

[a] The entries in columns 2−4 are parameters measured to the first amide group, whereas in columns 5−7, parameters measured to the second amide group are listed. The parameters of the weak C−H···O hydrogen bond (see Figure 3 for explanation) are given in columns 8−10. ΔR_{NH} and ΔR_{CH} are the bond elongations respectively contractions due to the hydrogen bonds. Therefore, the reference points are the corresponding distances of the isolated donors (100.5 pm for **IA** or **BA**, 100.6 pm for **PC**) The two last columns list the counterpoise corrected interaction energy E_I and the zero-point energy corrected interaction energy E_I^{ZPE} of each complex in kJ/mol. The complexes with the strongest binding energy are given first.

TABLE 2: Dipole Moment in Debye and Distances of the Acceptor C=O Bond Length in pm[a]

	2-fold						1-fold	
	μ_{tot}	μ_{acc}	μ'_{acc}	μ_{don}	R_{CO}	ΔR_{CO}	R_{CO}	ΔR_{CO}
IA	4.8			4.8				
3	10.8	3.8	3.5	4.4	124.2	1.7	123.4	0.9
2	10.8	4.4	4.2	4.4	122.9	1.3	122.3	0.7
1	10.2	4.1	4.0	4.4	122.1	1.0	121.8	0.7
4	9.5	3.1	3.0	4.5	121.9	0.8	121.6	0.5
5	8.3	2.4	2.4	4.5	120.6	0.4		
6	6.1	0.5	0.4	4.8	119.3	0.4		
PC	2.2			2.2				
8	8.3	4.1	4.0	2.3	123.4	1.1		
9	6.9	3.1	3.0	2.3	121.7	0.6		

[a] R_{CO} is the bond length in the complex, and ΔR_{CO} is the bond elongation compared to the isolated acceptor. Dipole moments are given for the total complex (μ_{tot}), the acceptor (μ_{acc}), and the donor (μ_{don}) in the constrained geometries (i.e., the geometries of the complex) and for the optimized acceptors (μ'_{acc}).

dimer) $\approx$ 19 kJ/mol[79]). The single hydrogen bonds (Figures 2 and 3) are not constrained by any sterical effects. In this case, donor and acceptor can arrange in an optimal geometrical manner, and it is seen (Table 1) that the more electronegative N−H donor leads to N···O bond lengths which are generally 45 pm shorter than those of the corresponding C···O unit.

To estimate the strength of the weak C−H···O hydrogen bond, we calculated the hydrogen bond complex depicted in Figure 3. We find a strength of the binding energy of 2 kJ/mol which is in the error range of our method. Therefore, we can only estimate that there is a slightly attractive contact, but refrain from a qualitative discussion of the binding energy. We also investigate intramolecular X−H bond elongation and contraction upon hydrogen bonding. The corresponding data are listed in Table 1 (ΔR_{NH} and ΔR_{CH}). We observe trends that are too small to be discussed quantitatively in light of the accuracy of the chosen method; that is, changes are within 0.5 pm. However, we can say that the hydrogen bond formation at the amide groups leads to bond elongation of the donor−proton bond, and the weak hydrogen bond at the C−H group yields a bond contraction. This is typical for red-shifted and blue-shifted hydrogen bonds and has been discussed extensively in the literature. For references to bond elongation in hydrogen bonds, see refs 2 and 4 and for discussion of the bond contraction see refs 2, 5, and 80. Comparing the 2-fold complexes with the complexes with single hydrogen bonds, we find slightly larger bond elongation for the N−H bond and much smaller effects for the C−H distance. The change of the carbonyl bond in the acceptor upon hydrogen bonding (Table 2) is also of interest. The 2-fold hydrogen-bonded complexes show a bond elongation of the carbonyl group by up to 1.7 pm. This elongation is stronger in the 2-fold hydrogen bond complexes than in the single bonded complexes.

The dipole moments of the complexes and of the separated units are given in Table 2. The dipole moments of the separated units acceptor and donor molecules are computed at the geometry the units hold in the complex. This is the origin for different values of the dipole moments at the same acceptor molecules; see acceptor molecules in complexes **1**−**6**. For the isolated **IA**, the total dipole moment is 4.8 D. For the complexes, the dipole moments are in the range of 6−10 D. They are related to the strength of the binding energy (i.e., show analogous trends). The vector of the dipole points in the direction of the acceptor oxygen, if we choose the middle C atom of the benzene ring (atom 6) as the origin of the calculation. The effect of forming a hydrogen bond for the donor molecule leads to a slight decrease of its dipole moment; see the third column Table 2. However, complexes **8** and **9** show a minor opposite trend. The dipole moments of the different acceptor molecules all exhibit values in the range of 2.4−4.4 D; the dipole moment of the acceptor molecule in complex **6** is rather small due to a more balanced electron distribution. Dannenberg investigated dipole moments of water clusters. He found significant polarization effects, such that a hydrogen bond cannot be described by electrostatic interactions only.[81] We find our hydrogen bonded complexes to behave similarly in this regard.

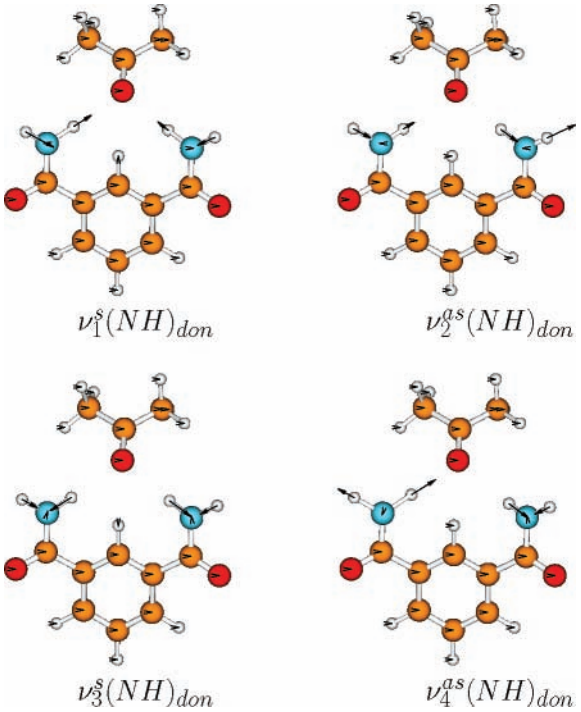

Figure 4. Visualized N−H frequencies at complex **4**.

4.2. Frequencies and Shifts. Characteristic modes are depicted in Figures 4−6. The N−H stretching modes occur in the region of 3500−3700 cm^{-1}, and the NH_2 bending modes are located between 1620 and 1660 cm^{-1}. The C−H stretch frequencies are calculated to be in the range around 3200 cm^{-1}. The bands of carbonyl stretching modes are of large interest because of their high intensities. In the investigated systems, we can distinguish between carbonyl stretching modes of the amide groups of the donor molecule, which are found between 1650 and 1750 cm^{-1}, and stretching modes of the acceptor. The latter occur depending on the acceptor molecule in the region of 1640−1870 cm^{-1} (1645 cm^{-1} for **3** and 1867 cm^{-1} for **6**). The frequencies of **7** are different than those of the complexes **1**−**6**. The stretching modes (ν_3^s(NH) and ν_4^{as}(NH)) (see Table 3) of **7** are located around 3200 cm^{-1} instead of around 3500 cm^{-1} as for the other complexes, because of the very strong anionic hydrogen bond.

Since the absolute values are not significant in this context, we focus our attention on the shifts of the frequencies. This means we discuss the difference between the calculated frequencies of the complex and the isolated molecules. The shifts of the complexes relative to the donor molecule are given in Tables 3−5. We observe red-shifts for the N−H stretching modes ν_1−ν_4 and blue shifts for the NH_2 bending modes; see Tables 3 and 4. The ν_1 and ν_2 bands are shifted by up to 30 cm^{-1}, whereas the ν_3 modes are shifted more by up to 50 cm^{-1} and the ν_4 bands by up to 60 cm^{-1}. We can identify two significant bending

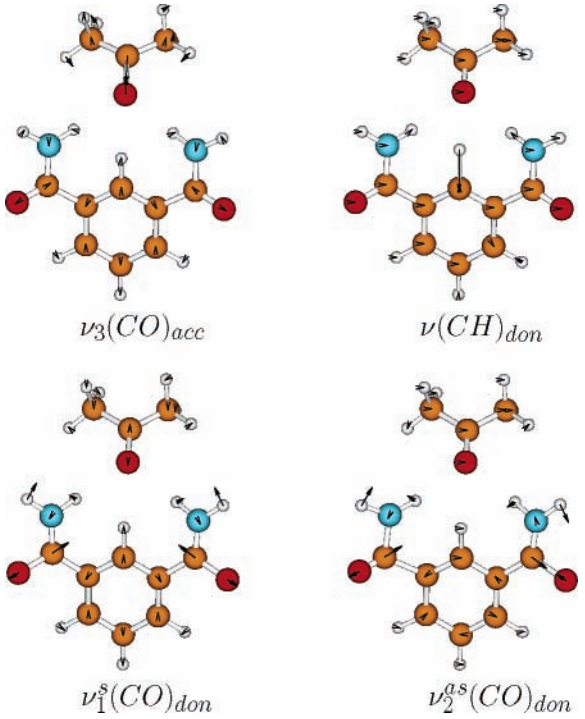

Figure 5. Visualized C−O and C−H frequencies at complex **4**. First panel: The C−O stretch of the acceptor and C−H stretch of the donor, lower panel: C−O stretch of donor; left: symmetric stretch; right: asymmetric stretch.

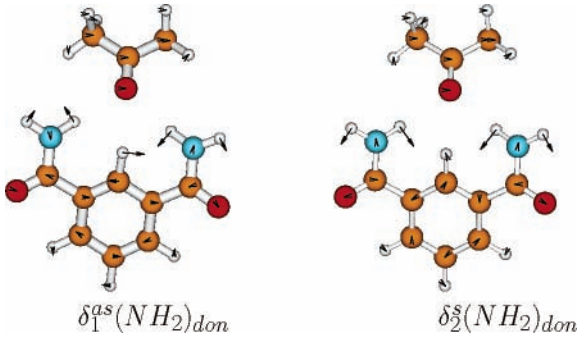

Figure 6. Visualized bending frequencies at complex **4**.

TABLE 3: Calculated Frequencies and Differences to the Corresponding Donor Molecule (e.g., IA for the First Block, in cm^{-1})[a]

	$\nu_1^s(NH)_{don}$	I	$\nu_2^{as}(NH)_{don}$	I	$\nu_3^s(NH)_{don}$	I	$\nu_4^{as}(NH)_{don}$	I
				IA and Complexes				
IA	3713	15	3711	58	3585	65	3583	22
3	−32	34	−32	140	−53	347	−60	116
2	−25	61	−28	123	−40	276	−49	108
1	−23	30	−24	155	−32	262	−39	67
4	−25	41	−25	147	−34	303	−38	27
5	−14	25	−15	145	−14	206	−17	5
6	−3	46	−5	75	−1	108	−3	31
7	−64	3	−62	69	−336	1520	−389	318
				PC and Complexes				
PC	3730	18	3725	159	3593	73	3588	3
8	−36	41	−40	112	−59	344	−78	200
9	−30	46	−32	127	−37	264	−48	128

[a] ν_1, ν_2, ν_3, and ν_4 are stretching modes of the amide N−H group from the donor molecule (don). Absolute intensities in km/mol. ν_1 and ν_3 are symmetric, and ν_2 and ν_4 are asymmetric.

modes of the NH_2 groups: the asymmetric δ_1 NH_2 mode and the symmetric δ_2 NH_2 mode depicted in Figure 6. We observe blue shifts up to 30 cm^{-1} for these modes.

TABLE 4: Calculated Frequencies and Differences to the Corresponding Donor Molecule (e.g., IA for the First Block, in cm^{-1})[a]

	$\nu_1^s(CO)_{don}$	I	$\nu_2^{as}(CO)_{don}$	I	$\delta_1^{as}(NH_2)$	I	$\delta_2^{s}(NH_2)$	I
IA	1754	283	1748	373	1641	6	1625	171
3	−16	310	−17	433	17	47	29	25
2	−14	146	−16	417	14	46	24	177
1	−13	535	−13	424	12	34	23	188
4	−12	477	−12	430	11	30	21	201
5	−9	333	−10	409	8	22	16	186
6	−5	328	−6	406	3	9	5	210
7							98	591
PC	1760	246	1753	405	-		1600	327
8	−11	252	−11	440	-		17	629
9	−12	477	−10	434	-		14	437

[a] $\nu_1^s(CO)_{don}$ and $\nu_2^{as}(CO)_{don}$ are modes of the carbonyl group of the donor molecule (don). $\delta_1^{as}(NH_2)$ and $\delta_2^{s}(NH_2)$ are bending modes of the NH_2 groups of the donor molecule. Absolute intensities in km/mol.

TABLE 5: Calculated Frequencies and Differences to the Corresponding Donor Molecule (e.g., IA for the First Block, in cm^{-1})[a]

	$\nu(CO)_{acc}$	I	$\nu(CH)_{don}$	I
IA			3179	5
3	−64	982	55	3
2	−39	1034	49	0.3
1	−29	501	48	0.3
4	−33	229	47	0.1
5	−17	169	36	0.4
6	−14	128	18	2
8	−35	540		
9	−22	151		

[a] $\nu(CO)_{acc}$ are the shifts (compared to the isolated molecule) from the carbonyl group of the acceptor. C−H denotes the stretch of the C−H group of the donor molecule. Absolute intensities in km/mol.

TABLE 6: Calculated Frequencies and Differences to Benzamide (BA) for Single Hydrogen Bond Complexes in cm^{-1}

	ν_1(NH)	I	ν_2(NH)	I	$\nu(CO)_{don}$	I
BA	3713	37	3587	44	1748	320
3−1	−39	109	−64	391	−16	287
2−1	−39	127	−60	374	−20	963
1−1	−31	106	−43	272	−19	463
4−1	−24	118	−29	243	−18	452
	$\nu(CO)_{acc}$	I	ν(CH)	I	$\delta(NH_2)$	I
BA			3196	10	1623	50
3−1	−31	654	7	3	27	274
2−1	−15	169	9	1	28	146
1−1	−25	549	9	2	28	130
4−1	−20	255	5	2	19	96

[a] $\nu(CO)_{acc}$ are the shifts (compared to the isolated molecule) from the carbonyl group of the acceptor. Absolute intensities in km/mol.

The C═O modes of the acceptor as well as of the donor are also red-shifted; see Tables 4 and 5. The largest shift for the acceptor is about 60 cm^{-1} which is also comparable to the largest N−H shift. However, the importance of the carbonyl bands is reflected in the large intensities they possess as compared to the N−H or the C−H modes. The red shift of the C═O stretching modes of the donor is smaller by up to 17 cm^{-1}. We also monitored the characteristic bands of the C−H···O group ν(CH). Here we observe a blue-shift in the range of 60 cm^{-1}.

Characteristic modes for the complexes with a single hydrogen bond are given in Table 6. The N−H stretching modes also occur in the region of 3500−3700 cm^{-1}, whereas the carbonyl

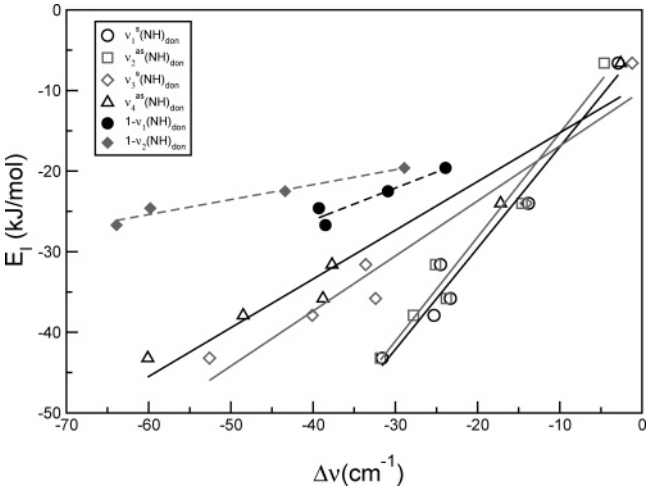

Figure 7. Interaction energy E_1 (kJ/mol) plotted against the N−H frequency shifts $\Delta\nu$ in cm^{-1}. The open symbols indicate the shifts as observed in the 2-fold hydrogen bonded complexes, and the filled symbols mark the shifts of the single-hydrogen bonded complexes.

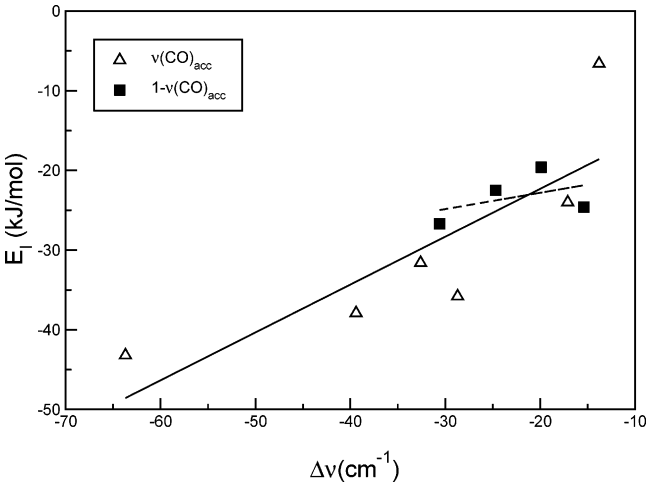

Figure 8. Interaction energy E_1 (kJ/mol) plotted against the C═O acceptor frequency shifts $\Delta\nu$ in cm^{-1}.

bands of the acceptor and donor are found between 1650 and 1750 cm^{-1}. The C−H stretch frequencies are located around 3200 cm^{-1}. $\delta(NH_2)$ shows around 1650 cm^{-1}.

It is possible to correlate the shifts of the frequencies for different complexes (**1** to **6** and **1-1** to **1-4**) to the character of the functional groups at the carbonyl oxygen. If we compare these complexes, we find the larger binding energy (i.e., the more electron donating groups at the nitrogen attached to the acceptor carbonyl carbon), the larger the shifts observed in the calculated spectrum. Accordingly, a plot of the frequency shifts versus the binding energy results in straight lines as can be taken from Figures 7−9. The red-shifts of the N−H bonds in **1**−**6** are well correlated to the energy of the hydrogen bond, see Figure 7. Although the slope of the correlation curve for the asymmetric stretch is rather large, the slope for the symmetric stretch is smaller for both the 2-fold hydrogen bond complexes as well as the single-bond complexes. Furthermore, the symmetric modes exhibit a wider ranges of shifts than the asymmetric shifts; the latter do not exceed −40 cm^{-1}. Comparing the 2-fold hydrogen-bonded complexes with the single hydrogen bonded, we find that the red-shifts are larger for the latter, whereas the slopes are steeper for the former.

The curves of the bending modes δ_1^{as} and δ_2^s (see Figure 9) show a similar course. However, in this case, we observe a

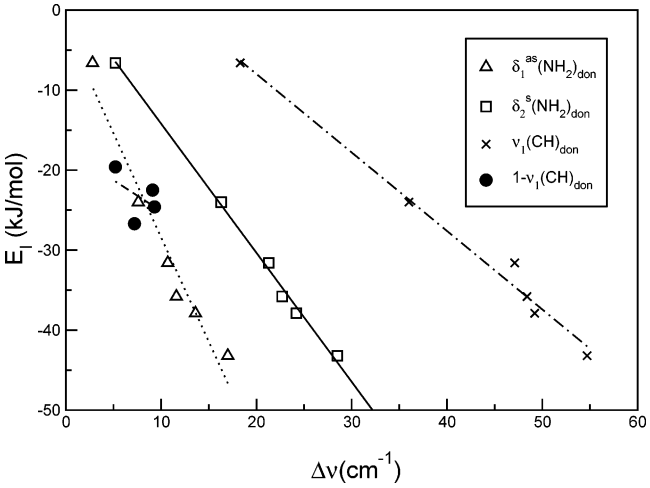

Figure 9. Interaction energy E_1 (kJ/mol) plotted against the frequency shifts $\Delta\delta$ of the NH_2 bending and $\Delta\nu$ of the C−H stretch in cm^{-1}.

TABLE 7: Parameter of the Linear Regressions of the Curves from Figures 7−9[a]

	m	b	x''	σ_s	σ_i	C
2-Fold Bonded						
$\nu_1^s(NH)_{don}$	1.257	−4.4	3713	0.116	2.59	0.98
$\nu_2^{as}(NH)_{don}$	1.291	−2.4	3711	0.119	2.38	0.98
$\nu_3^s(NH)_{don}$	0.683	−10.1	3585	0.094	3.14	0.96
$\nu_1^{as}(NH)_{don}$	0.605	−9.2	3583	0.077	3.03	0.97
$\delta_1^{as}(NH_2)$	−2.605	−2.4	1641	0.276	3.17	−0.98
$\delta_2^s(NH_2)$	−1.613	−1.9	1625	0.011	1.92	−1.00
$\nu(CH)_{don}$	−0.981	11.63	3179	0.058	2.57	−0.99
$\nu(CO)_{acc}$	0.601	−10.3		0.204	7.45	0.83
Single Bonded						
$\nu_1(NH)_{don}$	0.396	−10.2	3713	0.097	3.26	0.95
$\nu_2(NH)_{don}$	0.185	−14.3	3587	0.025	1.26	0.98
$\nu(CH)_{don}$	−0.772	−17.4	3196	0.976	7.69	−0.49
$\nu(CO)_{acc}$	0.205	−18.7		0.295	6.89	0.44

[a] m (in kJ/cm^{-1}) is the slope, and b (in kJ/mol) is the intercept of the straight lines. x'' (in cm^{-1}) is the reference point of the shifts, that means the value of the respective frequency of **IA** for the 2-folded and **BA** for the single bonded complexes. σ_s, σ_i, and C are the standard error of the slope respectively intercept and the correlation coefficient of the regression.

negative slope according to the blue shift of these modes. The bending modes $\delta(NH_2)$ for the single hydrogen bond likewise show a blue shift in the range of 25 cm^{-1}; however, the correlation of the shift to the interaction energy is not so pronounced. For the stretching modes of the donor carbonyl groups, we observe again red shifts which are correlated to the binding energy (see Table 4). These shifts are smaller (in the range of 5−15 cm^{-1}), because these groups are not directly involved at the hydrogen bonds.

The C═O shifts of the acceptor expose the same trends as the N−H stretching shifts, see Figure 8. Again we observe a wider range of frequency shifts (up to −65 cm^{-1}) for the 2-fold hydrogen bond complexes than for the single-bond hydrogen-bonded complexes, as well as steeper slope for the 2-fold hydrogen bond complexes. Compared to the other frequency shifts of the 2-fold bonded complexes, we notice a slightly larger deviation from the straight line in this case (see also Table 7). This may be caused by the fact that the other shift refers to the same donor (**IA**), whereas for this case, we always have different acceptors.

For the weak hydrogen bond contact between the acceptor oxygen and the middle C−H group of the donor, we find blue shifts up to 60 cm^{-1} for the corresponding C−H stretch mode. The minor influence of the C−H contact can also be gathered in Figure 9, where again the interaction energy is plotted against the frequency shift. Whereas in 2-fold hydrogen-bonded complexes the energy correlates well with the frequency shift, the same shift in the single hydrogen-bonded complexes is smaller and not so well related to the interaction energy. We detect blue shifts up to 10 cm^{-1}. This behavior can be explained by the fact that in complexes **1**−**6** the 2-folded hydrogen bond fixes the acceptor oxygen atom direct above the middle C−H group of the donor. At this a stronger 2-fold hydrogen bond leads to shorter O···N distances (see Table 1). As a consequence of this, the O···C distance (see eighth column of Table 1) is also shortened and the Pauli repulsion between the oxygen and the C−H group increases. According to Schlegel and co-workers, blue shifts of hydrogen bonds occur if the shortening of the X−H bond caused by the repulsive steric interaction between the involved atoms (Pauli repulsion) is larger than the bond elongation due to orbital interactions.[19] For the single bonded systems **1-1** to **4-1**, we do not observe such a large shortening of the O···C distance (see Table 1). Furthermore, the acceptor is not directly fixed above the C−H group. In Table 7, we present the parameters and the correlation coefficient of the linear regression of the curves from Figures 7−9. These data might be helpful for an estimation of the strength of 2-fold hydrogen bonds by means of infrared spectroscopy. The energy of the hydrogen bond can be evaluated by inserting the shift $\Delta x'$ in the equation $E = m\cdot\Delta x' + b$ or the absolute frequency x in the equation $E = m\cdot(x - x'') + b$, where x'' (in cm^{-1}) is the reference point for the calculation of the shifts, that means the value of the respective frequency of **IA** for the 2-fold and **BA** for the single bonded complexes.

For complex **7** the shifts are much larger due to the stronger hydrogen bond formed in this complex. The N−H modes ν_1^s(NH) and ν_2^{as}(NH) in this complex are shifted by approximately 60 cm^{-1}, whereas the ν_3^s(NH) and ν_4^{as}(NH) modes are shifted by 300−400 cm^{-1}. Furthermore, we observe a strong coupling of the ν_3^s(NH) and ν_4^{as}(NH) with the C−H stretch mode. We find such coupled frequencies at 3249, 3194, and 3185 cm^{-1}. Likewise, we calculate a large blue shift of 98 cm^{-1} for the $\delta_2^s(NH_2)$ mode ($\delta_1^{as}(NH_2)$ is difficult to assign in this case). The corresponding data point lies on the straight line for $\delta_2^s(NH_2)$ (see Figure 9) and was included in the linear regression analysis (see Table 7). The extreme large shifts of the N−H stretch modes can be attributed to a large charge-transfer of the anionic donor. As a result, the N−H bonds are weakened and therefore they are easier to excite.

The N−H shifts for the 2,6-pyridinedicarboxamide complexes **8** and **9** are comparable to the strongest carbonyl complex **3** and **2**. If we compare the data of **9** with that of **4** (both have the same acceptor molecule), we find more pronounced shifts for the pyridine complex **9**. At first glance, this is surprising, since **9** is not stronger bound (23.6 kJ/mol) than **4** (31.6 kJ/mol). On the other hand, the O···N distance (see Table 1) of **8** and **9** is the shortest of all which is an indication of a strong hydrogen bridge. However, its strength might be reduced by the geometric constraints which force an OHN angle of 156° and by the fact that the C−H group which forms a weak hydrogen bond in the other compounds is replaced in **8** and **9** by a nitrogen atom which possess a lone pair.

5. Conclusion

We calculated the IR shifts of the 2-fold hydrogen bond complexes. Although the hydrogen bonds are relatively weak, we do observe pronounced red shifts up to 65 cm^{-1} for the stretching modes of the acceptor carbonyl as well as for the donor NH_2 groups. The NH_2 bending modes $\delta_1^{as}(NH_2)$ and $\delta_2^s(NH_2)$ show a significant blue shift up to 30 cm^{-1}. We determined a linear correlation between the shifts of these bands and the interaction energy. Therfore, it should be possible to estimate the strength of 2-fold hydrogen bonds in complexes by inserting measured frequencies or shifts in the linear equations. We present the results of the linear regression analysis in Table 7. However, experimental identification of the modes is not trivial. Spectral shift could happen due to Fermi resonance, mixing of various modes, etc.[82] In particular, the NH_2 bending mode ($\delta_2^s(NH_2)$) should be suitable in this context because the corresponding graph shows a linear relationship over a wide range and their bands exhibit relatively high intensities (see Table 4). A comparison of the 2-fold and the single hydrogen bond complexes points out that the red shift of the N−H stretch is smaller for the 2-fold bonded systems. This is in accordance with the previous investigation where it was found that one hydrogen bond in the 2-fold hydrogen bond complexes is weaker than in the related single hydrogen-bonded complex.[38] However, for the C═O stretch mode of the acceptor carbonyl, we find an opposite trend. We observe a larger bond elongation of the C═O bond by up to 1.7 pm which is due to the fact that this group builds up two N−H···O hydrogen bonds (and in addition a weak C−H···O hydrogen bond). Accordingly, the red shift of these bands is larger than in the single bonded complexes. Hence, we can say that there is a smaller red-shift for the donor N−H stretch but a larger red-shift for the C═O acceptor stretch in a 2-fold hydrogen bond compared to a normal hydrogen bond.

What was not studied in our previous work is the weak hydrogen bond between the acceptor and the C−H group. Density functional calculations indicate that this bond is in the range of 2 kJ/mol, which is too small to be discussed quantitatively in light of the accuracy of density functional theory. Our calculation indicate that the corresponding C−H stretch mode will show a distinctive blue shift up to 55 cm^{-1} which is also directly correlated to the interaction energy. However, these bands exhibit only marginal intensities. The blue-shifts of the middle donor C−H bond are less pronounced in the single hydrogen bonded complexes than in the 2-fold complexes. Although the binding energy per contact is larger in the former (reflected in the larger red-shift for the N−H stretch), the C−H bond shifts are smaller and not so well correlated to the interaction energy for the single bonded complexes than for the 2-fold hydrogen bonded complexes. The reason for the pronounced blue shift of the C−H stretch is the specific geometrical arrangement of a 2-fold hydrogen bond which fixes the acceptor directly above the middle C−H group of **IA**. Finally, as discussed before for the geometries, it is obvious that the C−H contact must play a more important role in the 2-fold hydrogen-bonded complexes, since the carbonyl atom is shared between the two amide groups and the C−H group is just in its way. In the single hydrogen-bonded complexes the hydrogen bond can ideally arrange within the N−H···O═C group and gains 1.5 in interaction energy.

This study revealed the subtle features of hydrogen bonding in 2-fold hydrogen-bonded complexes from vibrational frequency calculations. We were able to determine different modes and learn about the individual shifts of this sort of special hydrogen bond. In the future, we hope to be able to transfer

this kind of study to the larger supramolecular complexes such as rotaxanes which are currently under investigation for instance in our collaborative research center "Templates".

Acknowledgment. We thank Wybren J. Buma for initiating the project and fruitful discussions. Financial support by the collaborative research center SFB 624 "Templates" at the University of Bonn is gratefully acknowledged.

References and Notes

(1) Arunan, E.; Klein, R. A. "IUPAC workshop "Hydrogen Bonding and Other Molecular Interactions", Pisa, Italy 5−9 September 2005", see also http://institut.physiochem.uni-bonn.de/IUPAC Pisa2005/Workshop.html.
(2) Kar, T.; Scheiner, S. *J. Phys. Chem. A* **2004**, *108*, 9161.
(3) Klein, R. A.; Mennucci, B.; Tomasi, J. *J. Phys. Chem. A* **2004**, *108*, 5851.
(4) Lakshmi, B.; Samuelson, A. G.; Jose, K. V. J.; Gadre, S. R.; Arunan, E. *New J. Chem*. **2005**, *29*, 371.
(5) Steiner, T.; Desiraju, G. R. *The weak hydrogen bond*; Oxford University Press: New York, 1999.
(6) Jäger, R.; Vögtle, F. *Angew. Chem*. **1997**, *109*, 967.
(7) Schalley, C. A.; Reckien, W.; Peyerimhoff, S. D.; Baytekin, B.; Vögtle, F. *Chem.—Eur. J*. **2004**, *10*, 4777.
(8) Seel, C.; Parham, A. H.; Safarofsky, O.; Hübner, G. M.; Vögtle, F. *J. Org. Chem*. **1999**, *64*, 7236.
(9) Hübner, G. M.; Gläser, J.; Seel, C.; Vögtle, F. *Angew. Chem*. **1999**, *111*, 395.
(10) Ghosh, P.; Mermagen, O.; Schalley, C. A. *Chem. Commun*. **2002**, *22*, 2628.
(11) Schalley, C. A.; Silva, G.; Nising, C. F.; Linnartz, P. *Helv. Chim. Acta* **2002**, 1578.
(12) Reuter, C.; Schmieder, R.; Vögtle, F. *Pure Appl. Chem.* **2000**, *72*, 2233.
(13) Biscarini, F.; Cavallini, M.; Leigh, D. A.; Leon, S.; Teat, S. J.; Wong, J. Zerbetto, F. *J. Am. Chem. Soc*. **2002**, *124*, 225.
(14) Pearson, R. G. *Chem. Rev.* **1985**, *85*, 42.
(15) Thar, J.; Kirchner, B. *J. Phys. Chem. A* **2005**, *110*, 4229.
(16) Pimentell, G. C.; McClellan, A. L. *The Hydrogen Bond*; Freeman: San Francisco, CA, 1997.
(17) Steiner, T.; Saenger, W. *J. Am. Chem. Soc.* **1993**, *115*, 4540.
(18) Budesinsky, M.; Fiedler, P.; Arnold, Z. *Synthesis* **1989**, 858.
(19) Li, X.; Liu, L.; Schlegel, H. B. *J. Am. Chem. Soc.* **2002**, *124*, 9639.
(20) van der Veken, B. J.; Herrebout, W. A.; Szostak, R.; Shchepkin, D. N.; Havlas, Z.; Hobza, P. *J. Am. Chem. Soc*. **2001**, *123*, 12290.
(21) Rutkowski, K. S.; Rodziewicz, P.; Melikova, S. M.; Herrebout, W. A.; van der Veken, B. J.; Koll, A. *Chem. Phys*. **2005**, *313*, 225.
(22) Kar, T.; Scheiner, S. *J. Phys. Chem. A* **2004**, *108*, 9161.
(23) Hobza, P.; Havlas, Z. *Chem. Rev.* **2000**, *100*, 4253.
(24) Chang, H. C.; Jiang, J. C.; Chuang, C. W.; Lin, S. H. *Chem. Phys. Lett.* **2004**, *397*, 205.
(25) Vijayakumar, S.; Kolandaivel, P. *J. Mol. Struct*. **2005**, *734*, 157.
(26) Chocholousova, J.; Spirko, V.; Hobza, P. *Phys. Chem. Chem. Phys.* **2004**, *6*, 37.
(27) Zierkiewicz, W.; Jurecka, P.; Hobza, P. *ChemPhysChem* **2005**, *6*, 609.
(28) Gu, Y.; Kar, T.; Scheiner, S. *J. Am. Chem. Soc.* **1999**, *121*, 9411.
(29) Scheiner, S.; Grabowski, S. J.; Kar, T. *J. Phys. Chem. A* **2001**, *105*, 10607.
(30) Scheiner, S.; Kar, T. *J. Phys. Chem. A* **2002**, *106*, 1784.
(31) Masunov, A.; Dannenberg, J. J.; Contreras, R. H. *J. Phys. Chem. A* **2001**, *105*, 4737.
(32) Hermansson, K. *J. Phys. Chem. A* **2002**, *106*, 4695.
(33) Bent, H. A. *Chem. Rev*. **1961**, *61*, 275.
(34) Alabugin, I. V.; Manoharan, M.; Peabody, S.; Weinhold, F. *J. Am. Chem. Soc*. **2003**, *125*, 5973.
(35) Reiher, M.; Kirchner, B. *J. Phys. Chem. A* **2003**, *107*, 4141.
(36) Reiher, M.; Sellmann, D.; Hess, B. A. *Theor. Chem. Acc.* **2001**, *106*, 379.
(37) Parthasarathi, R.; Subramanian, V.; Sathyamurthy, N. *J. Phys. Chem. A* **2006**, *110*, 3349.
(38) Reckien, W.; Peyerimhoff, S. D. *J. Phys. Chem. A* **2003**, *107*, 9634.
(39) Bünker, R. J.; Peyerimhoff, S. D. *Chem. Phys. Lett*. **1969**, *3*, 37.
(40) Bünker, R. J.; Peyerimhoff, S. D. *Theor. Chim. Acta* **1974**, *35*, 33.
(41) Bünker, R. J.; Peyerimhoff, S. D. *Theor. Chim. Acta* **1975**, *39*, 217.
(42) Morokuma, K.; Pedersen, L. J. *Chem. Phys.* **1968**, *48*, 3275.
(43) Dimitrova, Y.; Peyerimhoff, S. D. *Chem. Phys. Lett.* **1994**, *227*, 384.
(44) Dimitrova, Y.; Peyerimhoff, S. D. *Z. Physik* **1994**, *32*, 241.
(45) Marand, E.; Hu, Q.; Gibson, H. W.; Veytsman, B. *Macromolecules* **1996**, *29*, 2555.
(46) Gale, G. M.; Gallot, G.; Hache, F.; Lascoux, N.; Bratos, S.; Leicknam, J. C. *Phys. Rev. Lett.* **1999**, *82*, 1068.
(47) Asbury, J. B.; Steimel, T.; Stromberg, C.; Gaffney, K. J.; Piletic, I. R.; Groun, A.; Fayer, M. D. *Phys. Rev. Lett*. **2003**, *91*, 237402.
(48) Nie, B.; Stutzman, J.; Xie, A. *Biophys. J*. **2005**, *88*, 2833.
(49) Rubtsov, I. V.; Kumar, K.; Hochstrasser, R. M. *Chem. Phys. Lett*. **2005**, *402*, 439.
(50) Fecko, C. J.; Loparo, J. J.; andA. Tokmakoff, S. T. R. *J. Chem. Phys*. **2005**, *122*, 054506.
(51) Park, J.; Hochstrasser, R. M. *Chem. Phys*. **2006**, *323*, 78.
(52) Mikhaylova, Y.; Adam, G.; Haussler, L.; Eichhorn, K. J.; Voit, B. J. *Mol. Struct*. **2006**, *788*, 88.
(53) Wu, C. C.; Jiang, J. C.; Hahndorf, I.; Chaudhuri, C.; Lee, Y. T.; Chang, H. C. *J. Phys. Chem. A* **2000**, *104*, 9556.
(54) Kobko, N.; Dannenberg, J. J. *J. Phys. Chem. A* **2003**, *107*, 10389.
(55) Lu, J.; Zhou, Z.; Wu, Q.; Zhao, G. *J. Mol. Struct*. **2005**, *724*, 107.
(56) Bende, A.; Suhai, S. *Int. J. Quantum Chem*. **2005**, *103*, 841.
(57) Hayashi, T.; Zhuang, W.; Mukamel, S. *J. Phys. Chem. A* **2005**, *109*, 9747.
(58) Park, J.; Hochstrasser, R. M. *Chem. Phys.* **2006**, *323*, 78.
(59) Li, X.; Yang, D. *Chem. Commun.* **2006**, 3367.
(60) Grabowski, S. J.; Sokalski, W. A.; Leszcynski, J. *J. Phys. Chem. A* **2006**, *110*, 4772.
(61) Ha, J. H.; Kim, Y. S.; Hochstrasser, R. M. *J. Chem. Phys*. **2006**, *124*, 064508.
(62) Fanti, M.; Fustin, C. A.; Leigh, D. A.; Murphy, A.; Rudolf, P.; Caudano, R.; Zamboni, R.; Zerbetto, F. *J. Phys. Chem. A* **1998**, *102*, 5782.
(63) Larsen, O. F. A.; Bodis, P.; Buma, W. J.; Hannam, J. S.; Leigh, D. A.; Woutersen, S. *Proc. Natl. Acad. Sci. U. S. A.* **2005**, *102*, 13378.
(64) DeIonno, E.; Tseng, H. R.; Harvey, D. D.; Stoddart, J. F.; Health, R. *J. Phys. Chem. B* **2006**, *110*, 7609.
(65) Furer, V. L.; Borisoglebskaya, E. I.; Zverev, V. V.; Kovalenko, V. I. *Spectrochim. Acta Part A* **2006**, *63*, 207.
(66) Brouwer, A. M.; Frochot, C.; Gatti, F. G.; Leigh, D. A.; Mottier, L.; Paolucci, F.; Roffia, S.; Wurpel, G. W. H. *Science* **2001**, *291*, 2124.
(67) Becke, A. D. *Phys. Rev. A* **1988**, *38*, 3098.
(68) Becke, A. D. *J. Chem. Phys.* **1993**, *98*, 5648.
(69) The turbomole basis set library is available via anonymous ftp from ftp://ftp.chemie.uni-karlsruhe.de/pub/basen.
(70) Ahlrichs, R.; Bär, M.; Häser, M.; Horn, H.; Kölmel, C. *Chem. Phys. Lett*. **1989**, *162*, 165 Current version: see http://www.turbomole.de.
(71) Neugebauer, J.; Reiher, M.; Kind, C.; Hess, B. A. *J. Comput. Chem.* **2002**, *23*, 895.
(72) Sambrook, M. R.; Beer, P. D.; Wisner, J. A.; Paul, R. L.; Cowley, A. R.; Szemes, F.; Drews, M. G. B. *J. Am. Chem. Soc*. **2005**, *127*, 2292.
(73) Beer, P. D.; Sambrook, M. R.; Curiel, D. *Chem. Commun.* **2006**, 2105.
(74) Kavallieratos, K.; de Gala, S. R.; Austin, D. J.; Crabtree, R. H. *J. Am. Chem. Soc*. **1997**, *119*, 2325.
(75) Kavallieratos, K.; Bertao, C. M.; Crabtree, R. H. *J. Org. Chem.* **1999**, *64*, 1675.
(76) Bondy, C.; Loeb, S. J. *Coord. Chem. Rev*. **2003**, *240*, 77.
(77) Gale, P. A. *Acc. Chem. Res.* **2006**, *39*, 465.
(78) Schrader, T., Hamilton, A. D., Eds.; *Functional Synthetic Receptors*; Wiley-VCH: Weinheim, Germany, 2005.
(79) Kirchner, B. J. *Chem. Phys*. **2005**, *123*, 204116.
(80) Steiner, T.; Desiraju, G. R. *Chem. Commun.* **1998**, *8*, 891.
(81) Dannenberg, J. J. *J. Mol. Struct*. **2002**, *615*, 219.
(82) Herrebout, W. A.; Melikova, S. M.; Delanoye, S. N.; Rutkowski, K. S.; Shchepkin, D. N.; van der Veken, B. J. *J. Phys. Chem. A* **2005**, *109*, 3038.